Structural evolution of the $Z = 52$–62 neutron-deficient nuclei in the interacting boson approximation framework

S. Pascu,[1,2] N. V. Zamfir,[1] Gh. Căta-Danil,[1,2] and N. Mărginean[1]
[1]*National Institute for Physics and Nuclear Engineering, R-77125, Bucharest-Magurele, Romania*
[2]*Physics Department, University POLITEHNICA of Bucharest, R-060042, Romania*
(Received 30 March 2010; published 27 May 2010)

The interacting boson approximation (IBA) is employed in the present article to follow the structural evolution of the neutron-deficient nuclei from the $Z = 52$–62 region. The IBA model parameters are determined to reproduce the properties of the low-lying positive parity excitations for a wide range of even-even collective nuclei. The parameters aim to describe simultaneously the existing electromagnetic data (energy levels, transition matrix elements, etc.) and hadronic ones (two-nucleon transfer intensities). It is shown that a simple Hamiltonian with only two terms is not adequate to describe the properties across this region. It is found that the octupole term plays an important role in reproducing the properties of the 2^+_γ and 0^+_2 states, as well as in the description of the two-neutron transfer intensities patterns. A mapping of these parameters in the IBA symmetry triangle allows the comparison of representative trajectories for different isotopic chains.

DOI: 10.1103/PhysRevC.81.054321 PACS number(s): 21.10.Re, 21.60.Fw, 27.60.+j

I. INTRODUCTION

The interacting boson approximation (IBA) [1] has proven to be a valuable interpretive and predictive tool in understanding nuclear structure and its evolution along the isotopic and isotonic chains. The present article aims to investigate the changes in the structural evolution of Te, Xe, Ba, Ce, Nd, and Sm nuclei below $N = 82$. Most investigations carried out so far have focused on heavier isotopes because of the abundance of the available experimental data [2,3]. Recent studies provided detailed experimental information offering the possibility to study subtle changes in nuclear structure (see Refs. [4,5]).

The collective structure expected in these nuclei is ranging from vibrator for the Te isotopes ($Z = 52$) to axial rotor for the Sm isotopic chain ($Z = 62$). However, two of these neutron-deficient chains, namely Ba and Xe, are known to be unstable at γ deformation and were among the first regions assumed to have the O(6) symmetry in the IBA model [6]. To establish the structure of each isotopic chain from this region, detailed calculations of this region have to be carried out.

In the last decade, the IBA studies tried to describe the collective properties of the nuclei spanning a wide range of structures using a simplified Hamiltonian [2,7]. Recently, it was found that for Ba nuclei another term must be added in the model Hamiltonian to reproduce simultaneously the electromagnetic data and the hadronic ones [4,8]. Following this idea, the purpose of the present article is to analyze the complete spectroscopic properties of all low-lying positive parity excitations in the Te, Xe, Ba, Ce, Nd, and Sm isotopic chains using an extended Hamiltonian that includes also the octupole term. The obtained results are compared with the experimental values for each observable. Following the procedure from Ref. [2], a mapping of the employed parameters into the IBA symmetry triangle allows a comparison of the trajectories of each isotopic chain and a determination of their location relative to the well-known benchmarks of collective structure.

II. THEORETICAL FRAMEWORK

Calculations were performed in the IBA-1 framework (no distinction made between protons and neutrons) using the extended consistent Q formalism (ECQF) [9]. The Hamiltonian employed was [10]

$$\hat{H}_{sd} = \epsilon \hat{n}_d + \kappa(\hat{Q}\cdot\hat{Q})^{(0)} - 5\sqrt{7}\mathrm{OCT}[(\hat{d}^\dagger\tilde{d})^{(3)}\times[(\hat{d}^\dagger\tilde{d})^{(3)}]^{(0)}, \quad (1)$$

where $\hat{Q}$ is the quadrupole operator given by

$$\hat{Q} = [(\hat{s}^\dagger\tilde{d} + \hat{d}^\dagger\hat{s})^{(2)} + \chi(\hat{d}^\dagger\tilde{d})^{(2)}], \quad (2)$$

and ϵ, κ, χ, and OCT are the model parameters.

The quadrupole electromagnetic transition operator is

$$\hat{T}(E2) = e_2\hat{Q}, \quad (3)$$

where e_2 represents the boson effective charge [2].

The three dynamical symmetries of the IBA are given by the competition between the four parameters (ϵ, κ, χ, and OCT) of the Hamiltonian of Eq. (1) [10]. If N_B is the boson number and denote by ζ the ratio,

$$\zeta = \frac{4N_B}{4N_B + \frac{\epsilon}{\kappa}}, \quad (4)$$

and temporarily remove the octupole term from the present discussion, then the three dynamical symmetries are given by $\zeta = 0$ for U(5), ($\zeta = 1$, $\chi = -\sqrt{7}/2$) for SU(3), and ($\zeta = 0$, $\chi = 0$) for O(6). The transitional regions are described by diagonalizing the Hamiltonian for intermediate parameter values.

The quantities that represent key observables for the structure of collective even-even nuclei were taken into account in the present fits: the absolute values of the energies $E(2^+_1)$, $E(4^+_1)$, $E(2^+_\gamma)$, and $E(0^+_2)$, the absolute values of the electromagnetic transition probabilities (in W.u.), the $R_{2\gamma} = B(E2;2^+_\gamma \to 0^+_1)/B(E2;2^+_\gamma \to 2^+_1)$, and $R_{\gamma g} = B(E2;2^+_\gamma \to 0^+_1)/B(E2;2^+_1 \to 0^+_1)$ (although this ratio is

less precisely measured, so less emphasis was placed on reproducing these values) ratios were also considered.

Another observable that can be calculated within the IBA model is the binding energy, which can provide a sensitive test of the Hamiltonian used to fit entire isotopic chains. The quantities usually measured are not the energies themselves but rather two-neutron separation energies. These are defined as the difference in binding energies between nuclei differing by two neutrons (one boson). In this work, the two neutron separation energy is given [10]:

$$S_{2n}(N_B) = A + B \cdot N_B + BE(N_B + 1) - BE(N_B), \quad (5)$$

where $BE(\mathrm{N}_B)$ is the binding energy of the nucleus with N_B bosons; A and B are parameters taken as constants across a given isotopic chain.

As stated before, the goal of the present article is to describe simultaneously both the existing electromagnetic and the hadronic data. To achieve this goal, two-neutron transfer intensities between ground state of the target nucleus and the first excited states of the residual nucleus were also calculated. Although the model does not distinguish between proton and neutrons, two-nucleon transfer reactions have been treated by a formalism that takes somewhat into account these effects. The $L = 0$ transfer operator uses the leading order term proportional with the bosonic $\hat{s}$ operator [10]:

$$\hat{P}^{(0)}_{\nu} = \alpha_{\nu} \left(\Omega_{\nu} - N_{\nu} - \frac{N_{\nu}}{N} \hat{n}_d \right)^{\frac{1}{2}} \left(\frac{N_{\nu} + 1}{N + 1} \right)^{\frac{1}{2}} \hat{s}, \quad (6)$$

where Ω_{ν} is the pair degeneracy of neutron shell, N_{ν} is the number of neutron pairs, N is the total number of bosons, and α_{ν} is a constant parameter.

The two-neutron transfer intensity to the 2^+ states also offers important clues about the nuclear structure. For the $0^+_{g.s} \rightarrow 2^+$ transitions, the $L = 2$ transfer operator contains three different terms, proportional to the $\hat{d}^{\dagger}$, $\hat{s}^{\dagger}(\hat{d}^{\dagger}\tilde{d})^{(2)}$, and $(\hat{s}^{\dagger}\hat{s}^{\dagger}\tilde{d})$ operators [10]:

$$\hat{P}^{(2)}_{\nu,\mu} = \frac{N_{\nu} + 1}{N + 1} \left[\alpha \left(\Omega_{\nu} - N_{\nu} - \frac{N_{\nu}}{N} \hat{n}_d \right)^{\frac{1}{2}} \left(\frac{N_{\nu} + 1}{N + 1} \right)^{\frac{1}{2}} \hat{d}^{\dagger}_{\mu} + \beta \frac{(\Omega_{\nu} - N_{\nu})^{1/2}}{\sqrt{5}} \hat{s}^{\dagger}(\hat{d}^{\dagger}\tilde{d})^{(2)} + \gamma(\hat{s}^{\dagger}\hat{s}^{\dagger}\tilde{d}) \right], \quad (7)$$

where α, β, and γ are constant coefficients.

III. RESULTS OF THE IBA CALCULATIONS

Fits were performed for 53 collective even-even nuclei in the region with $Z = 52$–62 and $N = 66$–80. The experimental data are taken from Nuclear Data Sheets [11–23], except where noted.

Figure 1 summarizes the IBA parameters employed in the present study. Overall, the evolution of these parameters follows a smooth trend, accordingly to the gradual changes in nuclear structure. However, some nuclei have a different behavior, partially or throughout the entire isotopic chain. Typically, ϵ remain roughly at a constant value as neutron number increases up to $N \simeq 76$ then increases up to $N = 80$ as the nuclei evolve from rotational (midshell) to vibrational (near closed shell). The nuclei starts to show different behaviors for the quadrupole strength κ. The absolute values for the Te isotopes are much smaller than those for other nuclei and remain roughly at a constant value throughout this isotopic chain. The Sm nuclei follow a different trend having small absolute values for rotational nuclei (near midshell) and increasing absolute values as the isotopes evolve toward vibrational nuclei. The different trends in evolution of parameters for various isotopic chains is even more pronounced for the parameter χ. For the Te nuclei, the absolute value is large and approximately constant. The Xe-Nd isotopic chains are grouped near a constant value of $\chi \simeq -0.4$. The Sm nuclei, however, follow a completely different trend, as they start with large values for rotational nuclei and gradually approach (and even exceed) the $\chi \simeq -0.4$ value. The OCT parameter shows that this term is relatively large for increasing neutron number, although the parameter does not follow a regular trend. To reproduce the 0^+_2 states in Te isotopes, a term proportional with $(d^{\dagger}\tilde{d})^{(4)}$ was also introduced. The strength of this term is given by the HEX parameter [10] and was included in the fit only for Te nuclei. The effective value employed for HEX was ranging between 0 and 0.02 MeV.

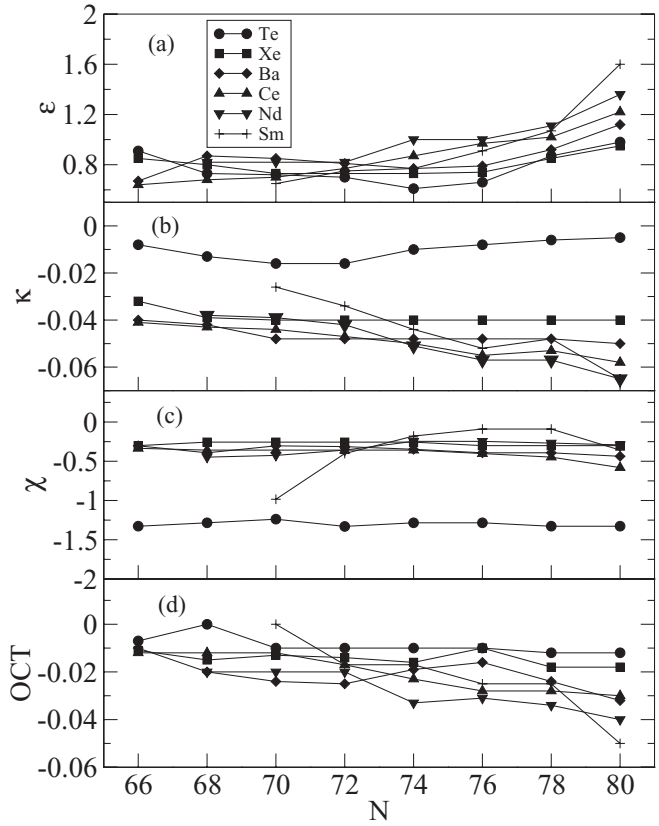

FIG. 1. Evolution of the ϵ, κ, χ, and OCT parameters for the Te-Sm isotopes as a function of neutron number. These values are obtained as a result of best fits of all collective observables. See text for details.

A fundamental observable to describe the structure of a nucleus is the $R_{4/2} = E(4^+_1)/E(2^+_1)$ energy ratio. The nuclei included in this study follow the expected trend of the evolution of the nuclear structure. They begin with a value that increases

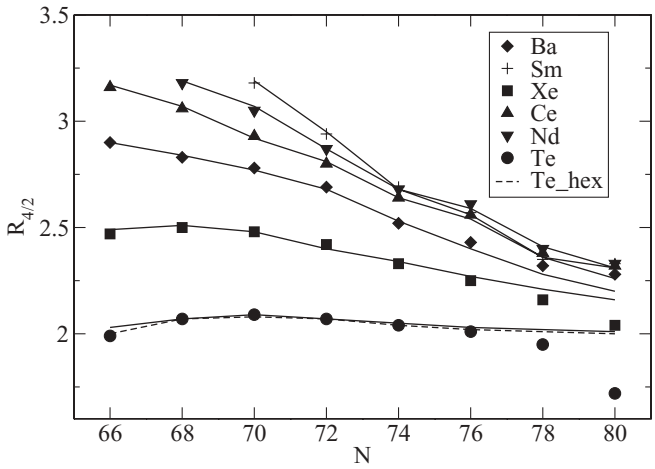

FIG. 2. Evolution of experimental (solid symbols) and theoretical (solid lines) $R_{4/2}$ values as a function of increasing neutron number. The dashed line shown for Te isotopes is calculated by including in the Hamiltonian the hexadecapole term given by the HEX parameter (see text for details).

with increasing Z and ranges from 2 (vibrational limit) for Te isotopes to $\simeq$3.3 (rotational limit) for Sm. Te and Xe isotopes show an interesting behavior, having a peak of this ratio at $N = 70$ and $N = 68$, respectively. All the other nuclei are smoothly decreasing toward a value around 2.5. The IBA calculations reproduce all these behaviors and the results are displayed in Fig. 2.

The calculated energy spectra are compared with the available experimental data for a sample of nuclei in Fig. 3, including an example of a nucleus from each isotopic chain. The calculations provide a good description of the low-lying spectra for a wide range of structures. Generally, the agreement is very good for the quasi-γ band, excepting the 3^+_γ state where there are discrepancies (especially in ^{138}Sm) in reproducing the staggering of this band. Probably this could be reproduced by using a cubic term [24]. Experimentally, a rather constant spacing with increasing spin is observed. For the $K = 0^+_2$ band the model generally overpredicts the location of the levels with spin $J = 2$ and 4, but gives a very good reproduction of the bandhead (0^+_2).

A comparison of the systematic of experimental and calculated energies of key states for the Te-Sm isotopic chains is presented in Fig. 4. The overall agreement is good. Some discrepancies appear when the nuclei are approaching $N =$ 80. The energy of the 2^+_γ state increases with increasing N for Te, Xe, and Ba nuclei, while undergoing a subtle change when passing to Ce and Nd where it has a minimum in energy at $N =$ 74. For Sm nuclei, this minimum is given by the calculations in the same point, but the absence of experimental data prohibits a definite assignment of this energy minimum. The energy of the 0^+_2 has different behaviors for each isotopic chain. For Te nuclei it has a maximum at $N = 76$, then decrease to $N = 80$. These energies are reproduced only if the hexadecapole term is taken into consideration in the fit (the dashed line in Fig. 4). Reproducing the evolution of 0^+_2 states was the main reason for introducing this term. In Xe nuclei, the 0^+_2 state has also

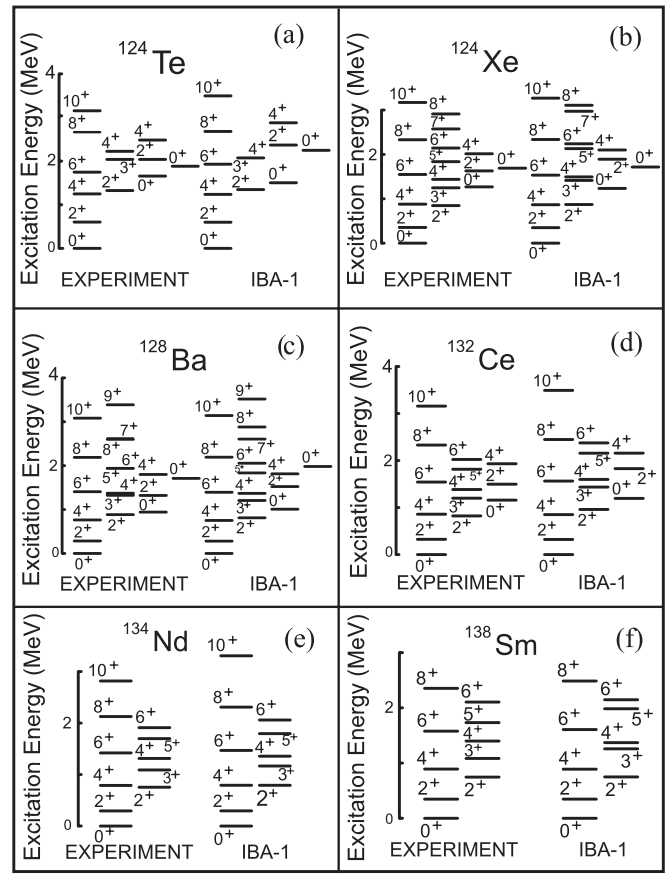

FIG. 3. Comparison between experimental and calculated energy levels for some nuclei in the Te-Sm region.

a maximum at $N = 78$, but the increase in energy is much smoother. In Ba and Ce isotopic chains, it has a minimum at $N = 72$, and for Nd and Sm no 0^+_2 is known at this time. The 0^+_3 states are well reproduced in Xe nuclei, whereas in Ba the trend is reproduced, although the absolute values of the experimental energies do not follow a very regular pattern.

Another fundamental observable that has to be reproduced by any theoretical calculations is the absolute value of the B(E2;$2^+_1 \rightarrow 0^+_1$) transition probability. To perform such calculations, the effective charge e_B from Eq. (3) was chosen such that it normalizes the predictions to the experimental value for one nucleus of each isotopic chain. The value determined in this way was kept at a constant value across the entire isotopic chain. The values increase as Z increases, ranging from 0.12 eb to 0.15 eb from Te to Sm, respectively. The results of the IBA calculations are displayed in Fig. 5. The agreement is good, with some exceptions. The experimental value at $N = 68$ in Te is much smaller than the others and cannot be reproduced by the model; in Xe isotopes, the experimental B(E2;$2^+_1 \rightarrow 0^+_1$) remain at a constant value for $N = 72$–76, while the calculations decrease smoothly.

Another sensitive structural quantity is the ratio $R_{2\gamma} = B(E2;2^+_\gamma \rightarrow 0^+_1)/B(E2;2^+_\gamma \rightarrow 2^+_1)$, which is 0 in the U(5) and O(6) limits and increases to the Alaga value of 0.7 in the rotational limit. As shown in Fig. 6, the experimental trend is excellent reproduced by the calculations. Most of the

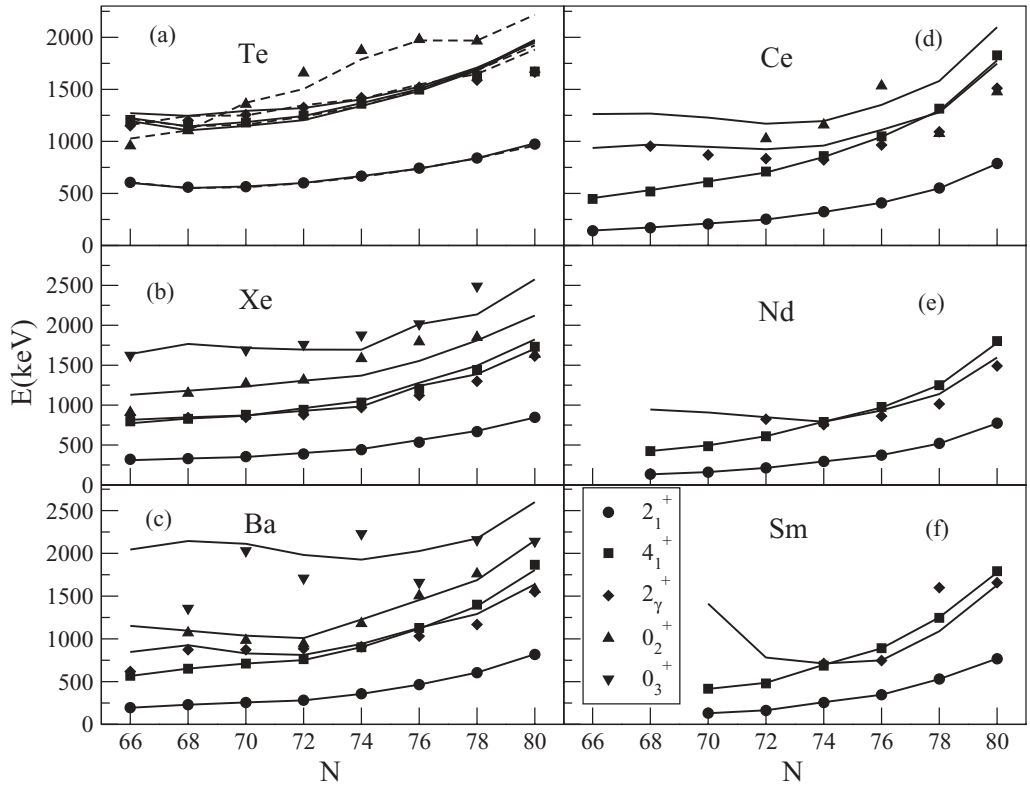

FIG. 4. Comparison of experimental level energies (symbols) and IBA calculations (solid lines) for the 2_1^+, 4_1^+, 2_γ^+, 0_2^+, and 0_3^+ states for Te, Xe, Ba, Ce, Nd, and Sm isotopes. Data are taken from Refs. [11–23], except for ^{130}Ba taken from Ref. [25]. The dashed lines shown for Te isotopes are calculated with the hexadecapole term included in the Hamiltonian of Eq. (1). The reproduction of the 0_2^+ states for these isotopes can only be achieved by including this term in the IBA calculations.

calculated values are within the experimental uncertainties. The inclusion of the octupole term in the Hamiltonian of Eq. (1) allowed the possibility of reproduction of both the experimental level energies and the experimental $R_{2\gamma}$ at the same time. Other choices of parameters (i.e., $\chi \simeq -1.0$) would result in energies for the 2_γ^+ and 0_2^+ states that overestimate by more than 500 keV the experimental values.

Other branching ratios, such as $B(E2;3_\gamma^+ \rightarrow 4_1^+)/B(E2;3_\gamma^+ \rightarrow 2_1^+)$, are also well reproduced by the present IBA calculations. This ratio goes to infinity in the

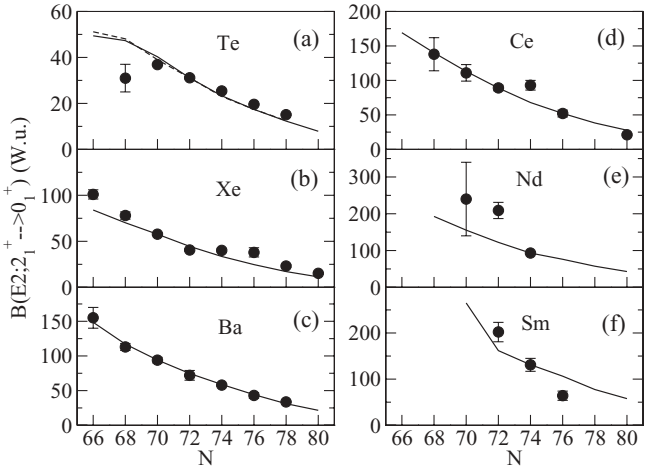

FIG. 5. Comparison between experimental (solid symbols) and IBA calculations (solid lines) for the B(E2;$2_1^+ \rightarrow 0_1^+$) transition probability. The dashed line for Te isotopes corresponds to inclusion of the hexadecapole term in the Hamiltonian of Eq. (1).

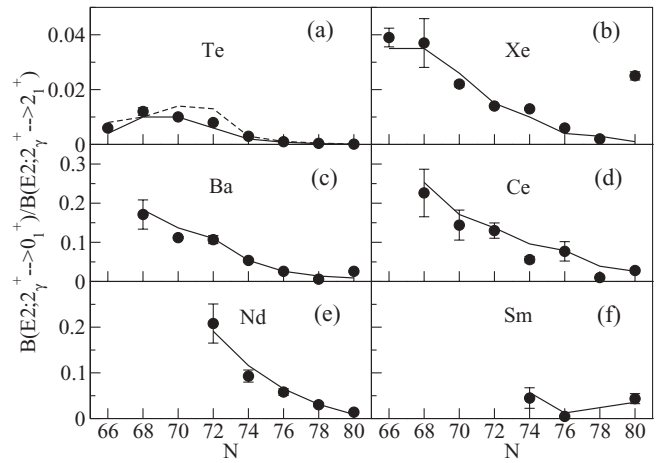

FIG. 6. Experimental $R_{2\gamma} = B(E2;2_\gamma^+ \rightarrow 0_1^+)/B(E2;2_\gamma^+ \rightarrow 2_1^+)$ ratios (solid symbols) and the IBA calculations (lines). The dashed line for Te isotopes corresponds to inclusion of the hexadecapole term in the Hamiltonian of Eq. (1).

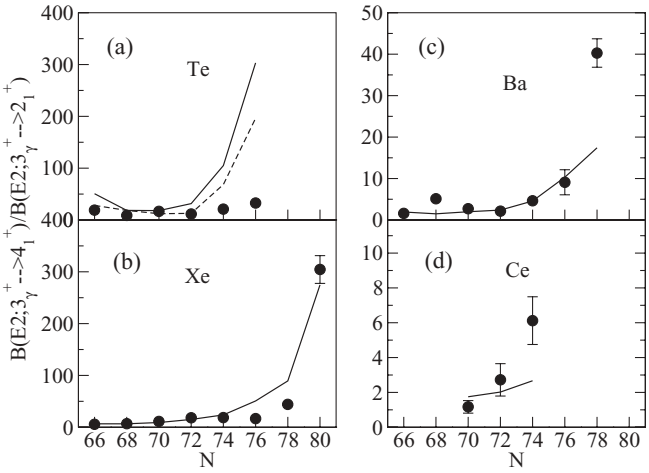

FIG. 7. Experimental $R_{3\gamma} = B(E2; 3^+_\gamma \to 4^+_1)/B(E2; 3^+_\gamma \to 2^+_1)$ ratios (solid symbols) and the IBA calculations (lines). The dashed line for Te isotopes corresponds to inclusion of the hexadecapole term in the Hamiltonian of Eq. (1).

U(5) and in the O(6) limits and to the Alaga value of 0.4 in the rotational limit SU(3). The results are presented in Fig. 7. The trend is overestimated by the calculations in heavier Te and Xe isotopes and slightly underestimated in Ba and Ce isotopes. Including the hexadecapole term in the calculations for Te isotopes (dashed line) gives a better prediction of the experimental values, but still overestimates the ratio for the large N.

With the energies of the 0^+_2 states reasonably described by the present calculations, the absolute transitions from these levels to the 2^+_1 states were also considered. Unfortunately, there are only four known absolute values (three in Te isotopes and one in Xe nuclei) for the $B(E2; 0^+_2 \to 2^+_1)$ transition probability. The results of the IBA calculations are displayed in Fig. 8. Although the agreement is not precise, the experimental trend is followed by the theoretical calculations.

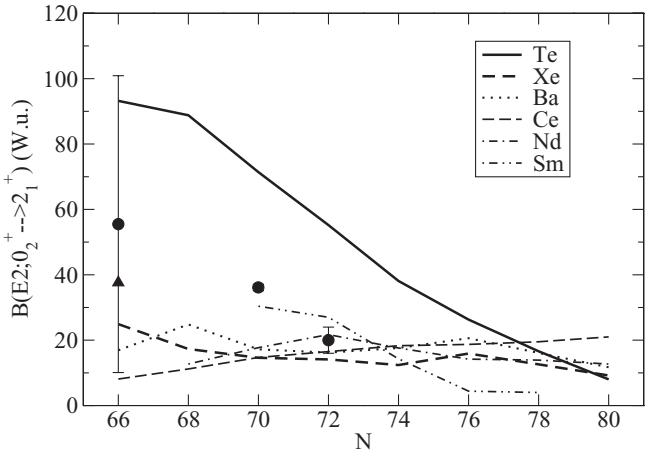

FIG. 8. Experimental $B(E2; 0^+_2 \to 2^+_1)$ transition probabilities (symbols) compared with the IBA calculations (lines). The solid circles correspond to Te isotopes and the triangle corresponds to the ^{120}Xe nucleus.

TABLE I. The IBA-1 parameters for Te-Sm isotopes employed in the two-neutron separation energy calculations.

Isotopic chain	A (MeV)	B (MeV)
Te	12.46	0.66
Xe	12.66	0.74
Ba	12.48	0.85
Ce	12.47	0.91
Nd	13.01	0.87
Sm	15.51	0.63

The importance of reproducing the two-neutron separation energies was stated before in Ref. [2]. Furthermore, in Ref. [26] it was found that it is possible to find IBA parameters that reproduce well the experimental energies but fail to reproduce the two-neutron separation energies. This quantity is considered to be a sensitive test for the applicability of the determined parameters to the entire isotopic chain. The present calculations are performed with the parameters given in Fig. 1 and with the additional parameters A and B of Eq. (5) given explicitly in Table I. The experimental values are taken from Ref. [27]. The comparison between the experiment and the calculated values is shown in Fig. 9.

In Refs. [4,8] it was stated that the addition of the octupole term in the Hamiltonian of Eq. (1) could describe simultaneously the electromagnetic data and the hadronic ones. Following this idea and using the present parameters determined for the entire isotopic chain, two-nucleon transfer intensities were calculated for ^{128}Ba-^{134}Ba nuclei. The experimental two-neutron transfer intensities are taken from Refs. [4,8,25] and are calculated as the factors used to normalize the distorted wave Born approximation (DWBA) curves to the experimental data. The calculated intensities are given by Eqs. (6) and (7). The intensities of the transitions to the 2^+ states are computed as a coherent sum of the three operators involved in Eq. (7). The comparison between the $2n$-transfer intensities and IBA predictions is given in Fig. 10 for the 0^+ states and in Fig. 11 for the 2^+ states. In the excitation range

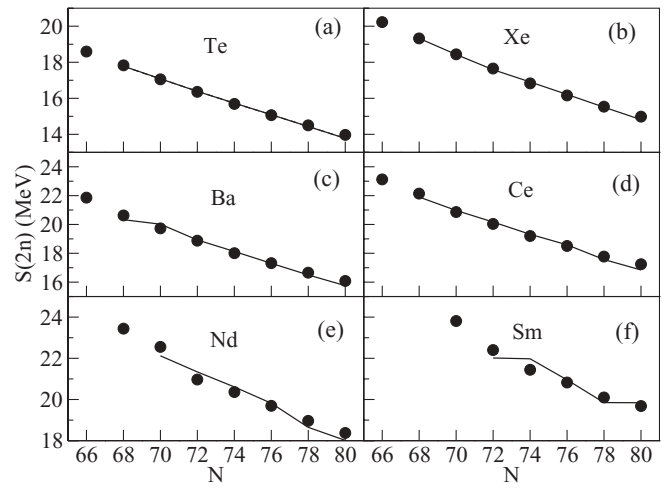

FIG. 9. Two-neutron separation energies for the Te-Sm region compared with the IBA calculations.

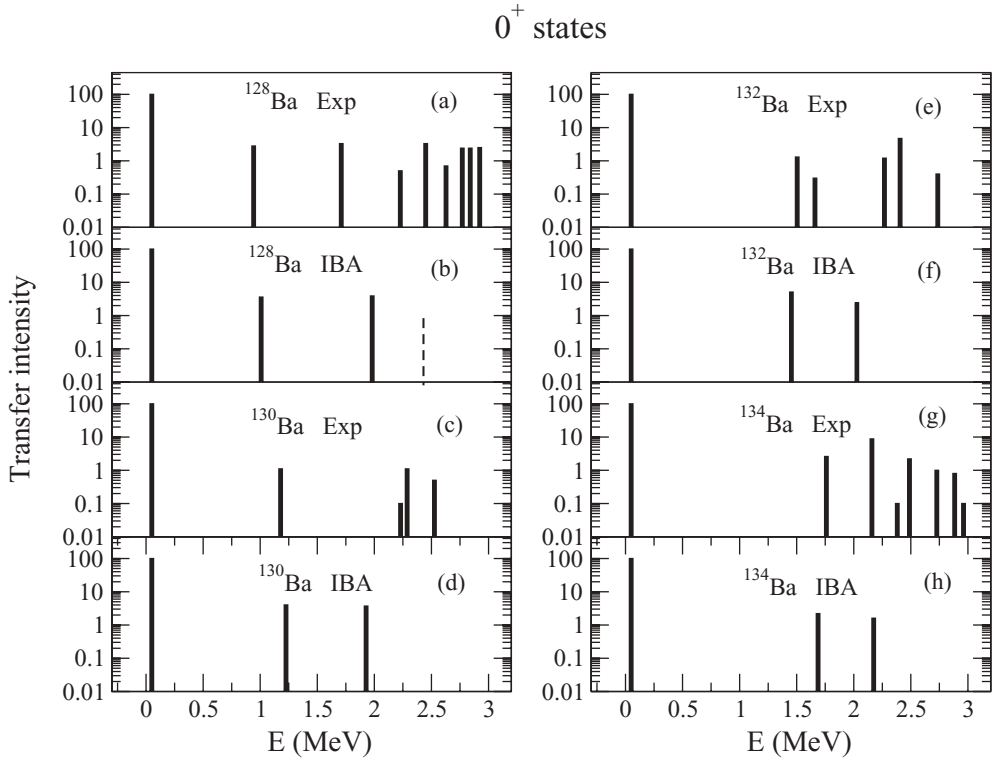

FIG. 10. Comparison of the experimental $L=0$ transfer intensities for the 0^+ states in the ^{128}Ba-^{134}Ba nuclei. The intensities are normalized to the 0_1^+(target) $\rightarrow$ 0_1^+(residual nucleus) transition. The vertical dashed line indicates only the energy of the next excited 0^+ state predicted by the IBA, but with a vanishing small (p,t) transfer intensity.

below 3 MeV, the calculations reproduce the (p,t) strengths for the first two excited states, both for $L=0$ and for $L=2$. Other states predicted by the IBA with less intensity are shown in Figs. 10 and 11 with dashed lines. These states do not have a clear correspondence with the experimental ones.

IV. MOTIVATION FOR USING THE OCTUPOLE TERM

Most of the IBA calculations have focused on reproducing only the electromagnetic properties of the studied nuclei (see, for example, Ref. [7]). The idea that simultaneous description of the hadronic (e.g., two-nucleon transfer intensities) and electromagnetic properties can give more insight to the nuclear structure has led the authors of Refs. [4,8] to perform calculations with an extended Hamiltonian in the consistent Q formalism (including the octupole term). In the present article there were calculated a wide range of nuclei spanning the $Z = 52$–62 region. From this point of view, we expect to find nuclei from vibrational [U(5)] limit to rotational [SU(3)] limit, passing near the γ-soft [O(6)] limit. This work showed that the octupole term is essential to describe simultaneously both the electromagnetic and hadronic properties of the nuclei. Moreover, the quality of the reproduction of the electromagnetic properties is also improved, becoming not only a qualitative description of the nucleus involved, but rather a quantitative reproduction of fundamental collective observables. The octupole term is indeed a useful tool in describing the data in this region as was demonstrated by Werner *et al.* [28] by introducing the second-order O(5) Casimir operator to account for the compression of τ multiplets in ^{124}Xe. The operator is diagonal and is used to remove the degeneration of the τ multiplets. More recently, experimental data [29] confirm the calculations performed in Ref. [28]. The present work uses this theoretical background and tries to describe the fundamental properties of a wide range of nuclei by employing a Hamiltonian that takes into account the second-order O(5) Casimir operator. The usage of the hexadecapole term is motivated only by means of pure phenomenological reasons to reproduce the energy of the 0_2^+ states in Te isotopes. The effect of considering a nonvanishing value for the OCT and HEX parameters on key observables for the structure of even-even nuclei can be observed from Table II. "Set 1" uses calculations performed with the parameters displayed in Fig. 1. "Set 2" takes the same values of the parameters as those used in "Set 1" except for the OCT parameter (and HEX), which is set to zero. From this comparison it can be observed that the collective observables are sometimes drastically affected by the absence of the octupole term. The effect of the OCT parameter is to increase the energy of the 0_2^+ state and to decrease the energy of the 2_γ^+ state. Furthermore, the ratios of the transition probabilities are improved by roughly a factor of five or more.

V. LOCATION OF THE NUCLEI IN THE IBA SYMMETRY TRIANGLE

The parameter space for the IBA Hamiltonian is generally represented by a triangle [9] with one dynamical symmetry at

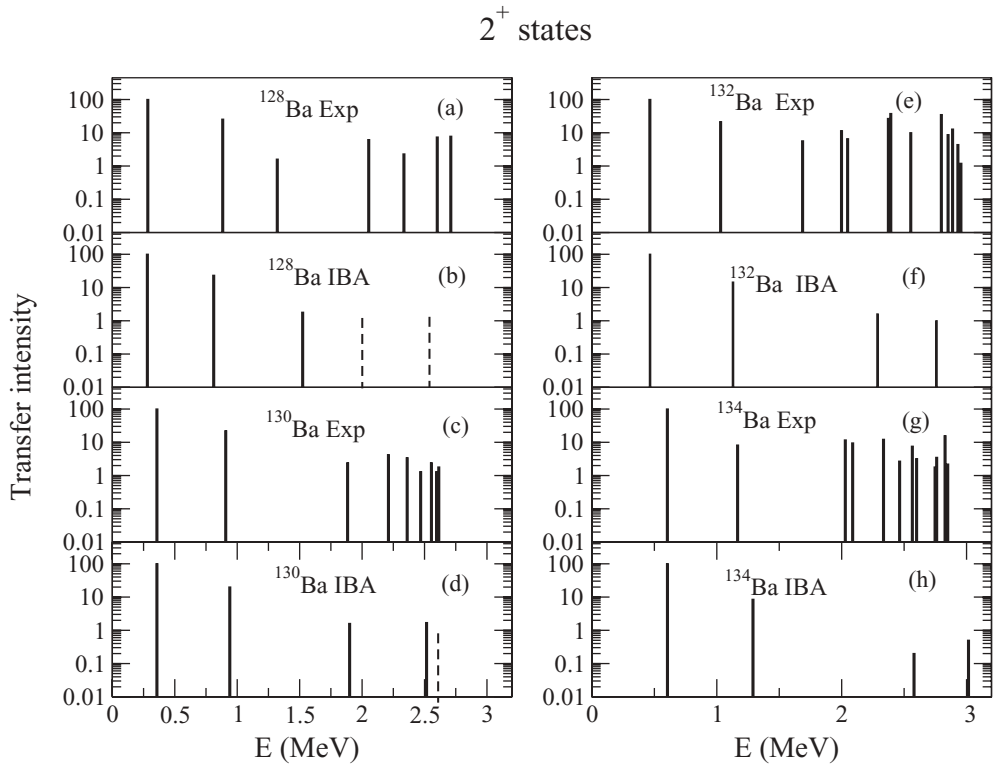

FIG. 11. Comparison of the experimental $L = 2$ transfer intensities for the 2^+ states in the ^{128}Ba-^{134}Ba nuclei. The intensities are normalized to the 0_1^+(target) $\rightarrow$ 2_1^+(residual nucleus) transition. The vertical dashed lines indicate only the energy of the next excited 2^+ states predicted by the IBA, but with vanishing small (p,t) transfer intensities.

each vertex. In Ref. [2] a simple procedure was introduced to obtain a pictorial view of the position of a nucleus in the symmetry triangle based on its IBA parameters. However, this procedure uses a simplified Hamiltonian in which only the first two terms from Eq. (1) are used. Because of the fact that the OCT parameter employed in the present article does not mix the basis states of the model, providing only a specific diagonal contribution, and because its value is always at most 15% (only for Nd and Sm; for the other isotopic chains this value is smaller than 5%) of that of the ϵ parameter (vibrational strength), the octupole term from Eq. (1) was neglected (because it is considered as a perturbation of the simplified Hamiltonian). In this way, the Hamiltonian takes a simple form, similar to the one used in Ref. [2] (with only two parameters, ζ and χ), and the procedure described can be applied. Having identified a set of parameters that provides a reasonable description of the low-lying states of the Te-Sm isotopic chains, the parameters ζ and χ can now be used to qualitatively establish the location of each nucleus inside the symmetry triangle. The obtained trajectories are shown in Fig. 12.

The trajectories of the Te-Sm isotopic chains show distinct behaviors. The Te nuclei lie very close to the U(5)–SU(3) leg of the symmetry triangle, as would be expected ($Z = 52$). The Xe-Ce region is spanning the U(5)–O(6) region of the triangle, having similar behaviors as N is increased. As it was already mentioned in the introduction, the Xe-Ba region is known to be unstable at γ deformation. In Ref. [6], the O(5) symmetry character has been demonstrated and it was proposed in that work that when the O(5) character is also present the O(6) symmetry might be a good symmetry. However, in Ref. [29] it was shown that for ^{124}Xe the O(6) symmetry is dissolved but the O(5) character remains, this later symmetry being slightly perturbed. The Ce isotopes are following a similar path along the U(5)–O(6) leg of the symmetry triangle. An interesting behavior is observed for Nd and Sm isotopes. As N decreases and consequently the boson number increases, the nuclei are not following the expected trend in becoming good axially rotors. The parameters involved in the present calculations places the Nd and Sm nuclei with a large neutron number ($N \geqslant 76$) along the U(5)–O(6) path. The turning point toward an axially symmetric rotor [SU(3) limit] appears at $N = 74$ for Nd and at $N = 76$ for the Sm nuclei. The absence of experimental data for light Nd and Sm nuclei prohibits for now a study of the further evolution.

Previous studies [30] have shown that when passing from vibrational to deformed shapes, a region of shape/phase coexistence exists. For $\chi \neq 0$, the phase/shape transition is of first order, whereas for $\chi = 0$ it converges to a single point, the critical point of second-order phase transition. According to Fig. 12, there are nuclei close to the second-order phase transition. Indeed, some of these nuclei have been proposed as candidates in which the phase/shape transition can occur. ^{134}Ba was the first nucleus proposed as having the second-order critical point symmetry [31]. For other nuclei (^{130}Xe, ^{132}Ba, etc.), fingerprints have also been found of a second-order phase

TABLE II. Comparison between the experimental values of key observables from one nucleus of each isotopic chain and the corresponding IBA values with two sets of parameters. Set 1 comprises the parameters given in Fig. 1. Set 2 takes the same values of the parameters as those used in Set 1 except for the OCT parameter (and HEX), which is set to zero.

Nucleus	Observable	Expt.	Set 1	Set 2
^{124}Te	$R_{4/2}$	2.07	2.07	2.10
	$E(0_2^+)/E(2_1^+)$	2.75	2.51	2.02
	$E(2_\gamma^+)/E(2_1^+)$	2.20	2.25	2.31
	$\frac{B(E2;2_\gamma^+\to 0_1^+)}{B(E2;2_\gamma^+\to 2_1^+)}$	0.0080(2)	0.013	0.012
	$\frac{B(E2;3_\gamma^+\to 4_1^+)}{B(E2;3_\gamma^+\to 2_1^+)}$	11.6(10)	12.8	16.4
	$B(E2;2_1^+\to 0_1^+)$ (W.u)	31.1(5)	31.1	33.7
	$B(E2;2_\gamma^+\to 0_1^+)$ (W.u)	0.49(5)	0.43	0.38
^{124}Xe	$R_{4/2}$	2.48	2.48	2.40
	$E(0_2^+)/E(2_1^+)$	3.58	3.53	3.33
	$E(2_\gamma^+)/E(2_1^+)$	2.39	2.49	2.55
	$\frac{B(E2;2_\gamma^+\to 0_1^+)}{B(E2;2_\gamma^+\to 2_1^+)}$	0.022(1)	0.026	0.001
	$\frac{B(E2;3_\gamma^+\to 4_1^+)}{B(E2;3_\gamma^+\to 2_1^+)}$	11.0(18)	9.11	20.82
	$B(E2;2_1^+\to 0_1^+)$ (W.u)	57.8(15)	57.7	58.2
	$B(E2;2_\gamma^+\to 0_1^+)$ (W.u)	0.7(1)	1.5	0.7
^{128}Ba	$R_{4/2}$	2.69	2.68	2.45
	$E(0_2^+)/E(2_1^+)$	3.32	3.59	3.50
	$E(2_\gamma^+)/E(2_1^+)$	3.11	2.89	2.71
	$\frac{B(E2;2_\gamma^+\to 0_1^+)}{B(E2;2_\gamma^+\to 2_1^+)}$	0.107(10)	0.110	0.02
	$\frac{B(E2;3_\gamma^+\to 4_1^+)}{B(E2;3_\gamma^+\to 2_1^+)}$	2.11(7)	2.39	12.0
	$B(E2;2_1^+\to 0_1^+)$ (W.u)	72(7)	74.7	76.3
	$B(E2;2_\gamma^+\to 0_1^+)$ (W.u)	3.4(6)	4.6	1.4
	$\epsilon(0_2^+)$	2.8(1)	3.6	5.0
	$\epsilon(0_3^+)$	3.3(2)	3.9	0.7
^{130}Ce	$R_{4/2}$	2.80	2.81	2.57
	$E(0_2^+)/E(2_1^+)$	4.04	4.69	4.17
	$E(2_\gamma^+)/E(2_1^+)$	3.29	3.71	3.19
	$\frac{B(E2;2_\gamma^+\to 0_1^+)}{B(E2;2_\gamma^+\to 2_1^+)}$	0.130(20)	0.137	0.04
	$\frac{B(E2;3_\gamma^+\to 4_1^+)}{B(E2;3_\gamma^+\to 2_1^+)}$	2.7(9)	2.0	5.5
	$B(E2;2_1^+\to 0_1^+)$ (W.u)	89(4)	88.9	
^{134}Nd	$R_{4/2}$	2.68	2.68	2.42
	$E(2_\gamma^+)/E(2_1^+)$	2.56	2.68	2.61
	$\frac{B(E2;2_\gamma^+\to 0_1^+)}{B(E2;2_\gamma^+\to 2_1^+)}$	0.093(13)	0.116	0.013
	$B(E2;2_1^+\to 0_1^+)$ (W.u)	93(3)	93.1	95.9
^{136}Sm	$R_{4/2}$	2.69	2.68	2.49
	$E(2_\gamma^+)/E(2_1^+)$	2.80	2.74	2.70
	$\frac{B(E2;2_\gamma^+\to 0_1^+)}{B(E2;2_\gamma^+\to 2_1^+)}$	0.045(23)	0.057	0.016
	$B(E2;2_1^+\to 0_1^+)$ (W.u)	131(14)	131.2	133.8

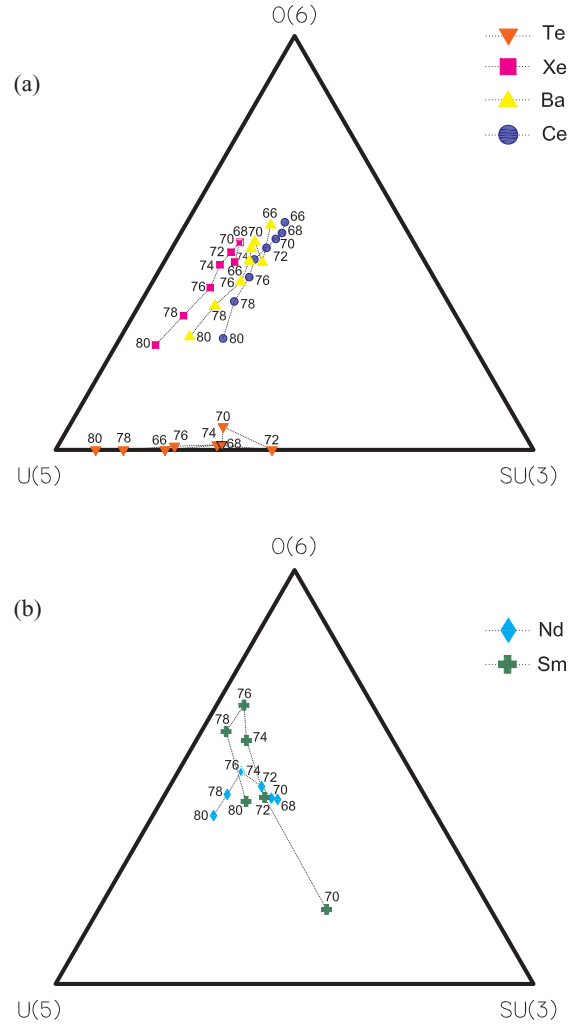

FIG. 12. (Color online) Trajectories in the IBA symmetry triangle for the Te-Sm isotopic chains. The trajectories are calculated using the simplified form of the Hamiltonian from Eq. (1) (OCT set to zero). The influence of the OCT parameter was discussed in Table II. For the present discussion, it was considered as a perturbation to the simplified Hamiltonian and was neglected.

transition [32]. The present calculations support this idea, placing these nuclei very close to the phase/shape transition region. The nucleus ^{128}Xe, which was proposed as having the E(5) symmetry in Ref. [32], was proven recently as not being a close realization of this critical point symmetry [33], in full agreement with the present calculations.

VI. CONCLUSIONS

Systematic IBA-1 calculations were performed for the $Z = 52$–62 and $N = 66$–80 region of collective even-even nuclei. It was shown that the simple Hamiltonian with only two terms is not adequate to describe the properties across the entire region. It was found that the octupole term plays an

important role in reproducing simultaneously electromagnetic and hadronic properties of the low-lying collective states. The calculations reproduce well the energies of key low-lying states and provide a good description of the electromagnetic transition strengths. An equal emphasis was placed on also reproducing the two-neutron transfer intensities, which brings additional evidence to establish the structure of a nucleus. The two-neutron separation energy is also well described. The obtained parameters corresponding to each nucleus were plotted into the IBA symmetry triangle using a set of polar coordinates. The trajectories are found to lie close to the vibrational limit [U(5)] for Te isotopes, passing near O(6) for Xe, Ba, and Ce nuclei, and going toward the rotational limit [SU(3)] for Nd and Sm isotopes.

ACKNOWLEDGMENTS

This work was supported in part by the National Council for Scientific Research in Higher Education (CNCSIS) under Contract Nos. ID-117/2007, ID-118/2007, and ID-180/2007, and by the National Centre for Programme Management (CNMP) under Contracts Nos. PNCDI II 71-042/2007, 71-051/2007, and 24EU-ISOLDE/2009.

[1] A. Arima and F. Iachello, Phys. Rev. Lett. **35**, 1069 (1975).
[2] E. A. McCutchan, N. V. Zamfir, and R. F. Casten, Phys. Rev. C **69**, 064306 (2004).
[3] O. Sholten, F. Iachello, and A. Arima, Ann. Phys. **115**, 325 (1978).
[4] S. Pascu *et al.*, Phys. Rev. C **79**, 064323 (2009).
[5] A. F. Mertz *et al.*, Phys. Rev. C **77**, 014307 (2008).
[6] R. F. Casten and P. von Brentano, Phys. Lett. B **152**, 22 (1985).
[7] W. T. Chou, N. V. Zamfir, and R. F. Casten, Phys. Rev. C **56**, 829 (1997).
[8] S. Pascu *et al.*, Phys. Rev. C **81**, 014304 (2010).
[9] R. F. Casten and D. D. Warner, Rev. Mod. Phys. C **60**, 389 (1988).
[10] F. Iachello and A. Arima, *The Interacting Boson Model* (Cambridge University Press, Cambridge, 1987).
[11] K. Kitao, Nucl. Data Sheets **75**, 99 (1995).
[12] K. Kitao, Y. Tendow, and A. Hashizume, Nucl. Data Sheets **96**, 241 (2002).
[13] T. Tamura, Nucl. Data Sheets **108**, 455 (2007).
[14] J. Katakura and Z. D. Wu, Nucl. Data Sheets **109**, 1655 (2008).
[15] J. Katakura and K. Kitao, Nucl. Data Sheets **97**, 765 (2002).
[16] M. Kanbe and K. Kitao, Nucl. Data Sheets **94**, 227 (2001).
[17] B. Singh, Nucl. Data Sheets **93**, 33 (2001).
[18] Yu. Khazov, A. A. Rodionov, S. Sakharov, and B. Singh, Nucl. Data Sheets **104**, 497 (2005).
[19] A. A. Sonzogni, Nucl. Data Sheets **103**, 1 (2004).
[20] A. A. Sonzogni, Nucl. Data Sheets **95**, 837 (2002).
[21] A. A. Sonzogni, Nucl. Data Sheets **98**, 515 (2003).
[22] N. Nica, Nucl. Data Sheets **108**, 1287 (2007).
[23] J. K. Tuli, Nucl. Data Sheets **89**, 641 (2000).
[24] N. V. Zamfir and R. F. Casten, Phys. Lett. B **260**, 265 (1991).
[25] G. Suliman *et al.*, Eur. Phys. J. A **36**, 243 (2008).
[26] J. E. Garcia-Ramos *et al.*, Nucl. Phys. A **383**, 264 (1982).
[27] G. Audi, A. H. Wapstra, and C. Thibault, Nucl. Phys. A **729**, 337 (2003).
[28] V. Werner *et al.*, Nucl. Phys. A **692**, 451 (2001).
[29] G. Rainovski *et al.*, Phys. Lett. B **683**, 11 (2010).
[30] F. Iachello, N. V. Zamfir, and R. F. Casten, Phys. Rev. Lett. **81**, 1191 (1998).
[31] R. F. Casten and N. V. Zamfir, Phys. Rev. Lett. **85**, 3584 (2000).
[32] R. Rodriguez-Guzmán and P. Sarriguren, Phys. Rev. C **76**, 064303 (2007).
[33] L. Coquard *et al.*, Phys. Rev. C **80**, 061304(R) (2009).